Calculating Kelvin force microscopy signals from static force fields

Lukasz Borowik, Koku Kusiaku, Didier Theron, Thierry Melin

Calculating Kelvin force microscopy signals from static force fields

Cite as: Appl. Phys. Lett. **96**, 103119 (2010); https://doi.org/10.1063/1.3323098
Submitted: 17 November 2009 • Accepted: 26 January 2010 • Published Online: 12 March 2010

Łukasz Borowik, Koku Kusiaku, Didier Théron, et al.

Calculating Kelvin force microscopy signals from static force fields

Łukasz Borowik, Koku Kusiaku, Didier Théron, and Thierry Mélin[a)]
Institute of Electronics, Microelectronics, and Nanotechnology, CNRS, UMR 8520, Avenue Poincaré, BP 60069, 59652 Villeneuve d'Ascq Cedex, France

(Received 17 November 2009; accepted 26 January 2010; published online 12 March 2010)

We present an analytical formula to achieve numerical simulations of Kelvin force microscopy (KFM) signals from static force fields, which can be employed to describe amplitude-modulation or frequency-modulation KFM, as well as simultaneous topography and KFM modes for which the tip probe exhibits a nonzero oscillation during KFM imaging. This model is shown to account for side-capacitance and nonlinear effects taking place in KFM experiments, and can therefore be used conveniently to extract quantitative information from KFM experiments at the nanoscale. © *2010 American Institute of Physics*. [doi:10.1063/1.3323098]

The ability to measure local surface potentials at the nanoscale is essential for material science, nanoelectronics, and nanotechnology. The most common technique for such measurements is Kelvin force microscopy (KFM), which uses the cantilever of an atomic force microscope as a Kelvin probe.[1] Numerous variants of KFM have been developed since the 1990s, in which the surface potential is either detected in air or in a vacuum environment,[2] either separately or simultaneously with the topography imaging,[3] and finally either using force or force gradient signals leading, respectively, to amplitude-modulation KFM (AM-KFM) or frequency-modulation KFM (FM-KFM). All implementations however suffer from the fact that the cantilever tip probes actually "feel" the surface through a series of parallel capacitances. This averaging effect both degrades the lateral resolution in KFM and prevents direct quantitative measurements of surface potentials as first analyzed by Jacobs *et al.*[4] This issue is already significant at the micrometer[5] or submicrometer[6] scale due to the capacitive interaction of the cantilever itself with the surface but becomes especially relevant when imaging features below the tip apex radius,[7,8] or at the nanoscale. Although a phenomenological description may be obtained from experiments,[9] the extraction of the real local electrostatic potentials from KFM data needs in general to be performed through simulations.[4,10]

In this letter, we present an analytical formula to achieve numerical simulations of KFM signals *from static force fields*, which can be used either for AM-KFM or FM-KFM. The model is shown to conveniently account for side-capacitance effects,[4] and thus, to enable the extraction the real electrostatic potentials from measured KFM signals, even at the nanometer scale. It is also generalized to the case of an oscillating tip probe. This corresponds to experimental situations in which the tip probe is, e.g., mechanically excited at its fundamental resonance and electrostatically excited either at low frequency or at a cantilever higher-order resonance so as to simultaneously determine either FM-KFM or AM-KFM signals,[2,3,11,12] respectively. Our model enables us to take into account the nonlinearities of surface potentials with the tip-substrate distance, which are crucial to interpret KFM experiments performed at short (i.e., less than 20 nm) tip-substrate distances, such as in atomically resolved noncontact atomic force microscopy.

The basic principle of KFM (here AM-KFM) between a tip probe set at a distance z from a sample of surface potential V_S consists of: (i) applying a dc+ac bias $V_{dc}+V_{ac}\sin(\omega t)$ to the tip forming a capacitance $C(z)$ with the sample; (ii) monitoring the cantilever capacitive force component along the z-axis $F_\omega(t)=\partial C/\partial z(V_{dc}-V_S)V_{ac}\sin(\omega t)$ at the excitation angular frequency ω (in practice, the cantilever oscillation at the angular frequency ω); and (iii) regulating the dc bias V_{dc} to nullify F_ω using a feedback loop. This provides a measurement of the sample surface potential V_S, which is here described in a purely capacitive model. In reality, V_S accounts for the work function difference between the tip and sample, but also for local electrostatic potentials, and for fixed charge or dipole contributions at the tip or at the sample surface. FM-KFM (resp. AM-KFM) experiments are based on force gradients (resp. forces) so that the regulation signal for the KFM loop is proportional to $\partial^2 C/\partial z^2$ (resp. $\partial C/\partial z$). In the following, we will address the particular case in which V_S only originates in a surface charge Q, but our analysis would be generalized readily to account for local changes in work function, electrostatic potentials, charge displacements, and surface dipoles.

To derive an expression of the dc potential regulated by a KFM loop (here, AM-KFM), we start from the total force F_{tot} at the tip (including its static, ω and 2ω components), which is written as $F_{tot}=1/2\varepsilon_0\int\int E_{tot}^2 dS$ when integrating the total electric field E_{tot} over the tip and cantilever surface. E_{tot} can be written as $E_{tot}=E_Q+E_{dc}+E_{ac}\sin\omega t$, in which E_Q is the electric field in presence of the charge Q but with the tip at zero bias, and $E_{dc}+E_{ac}\sin\omega t$ the electric field generated by the tip electrostatic excitation $V_{dc}+V_{ac}\sin(\omega t)$ and for $Q=0$. E_Q and $E_{dc}+E_{ac}\sin\omega t$ are by essence force fields with different topologies, since they correspond to image charge forces and to capacitive forces, respectively. The force component at ω equals $F_\omega(t)=F_\omega\sin(\omega t)$, in which F_ω equals

$$F_\omega=\varepsilon_0\iint E_{dc}E_{ac}dS+\varepsilon_0\iint E_Q E_{ac}dS. \quad (1)$$

The aim is now to express the force component F_ω from the *static* force fields which can be calculated independently using a Poisson solver: $F_{V_{stat}\neq 0,Q\neq 0}$, $F_{V_{stat}=0,Q\neq 0}$, and $F_{V_{stat}\neq 0,Q=0}$ obtained when a static bias V_{stat} is applied to the tip and/or a charge Q is present on the surface. The first term in Eq. (1) only includes capacitive electric fields (E_{dc} and E_{ac}) and can thus be directly written as

a)Electronic mail: thierry.melin@isen.iemn.univ-lille1.fr.

$2(V_{ac}V_{dc}/V_{stat}^2)F_{V_{stat}\neq 0,Q=0}$. The second term consists in an integrated product of the capacitive and image electric fields. The computational difficulty associated with this product can be circumvented since it also corresponds to the double product of $F_{V_{stat}\neq 0,Q\neq 0}=1/2\varepsilon_0\int\int(E_{stat}+E_Q)^2dS$ multiplied by V_{ac}/V_{stat}. By developing this equation, the second term in Eq. (1) thus becomes $V_{ac}/V_{stat}\times[F_{V_{stat}\neq 0,Q\neq 0}-F_{V_{stat}\neq 0,Q=0}-F_{V_{stat}=0,Q\neq 0}]$. The KFM condition $F_\omega=0$ then reads:

$$2(V_{dc}/V_{stat})F_{V_{stat}\neq 0,Q=0}+[F_{V_{stat}\neq 0,Q\neq 0}-F_{V_{stat}\neq 0,Q=0}-F_{V_{stat}=0,Q\neq 0}]=0. \quad (2)$$

It leads to the following expression for the surface potential V_{dc}, here noted $V_{dc}|_{AM-KFM,A=0}$ as it is determined for an AM-KFM loop with zero tip oscillation amplitude (A=0):

$$V_{dc}|_{AM-KFM,A=0}=-V_{stat}\times[F_{V_{stat}\neq 0,Q\neq 0}-F_{V_{stat}\neq 0,Q=0}-F_{V_{stat}=0,Q\neq 0}]/2F_{V_{stat}\neq 0,Q=0}. \quad (3)$$

This expression can be used to conveniently calculate surface potentials using a Poisson solver. Keeping in mind that V_{dc} is a phenomenological description of the total electrostatic force $F_{V_{stat}\neq 0,Q\neq 0}$ in the form of $A+B\times(V_{stat}-V_{dc})^2$, Eq. (3) can be also understood as the cross-term interaction between the surface charge Q and capacitive charges at the tip (double product in the previous expression, and hence, the force $F_{V_{stat}\neq 0,Q\neq 0}$ when corrected from the purely capacitive and image charge force components $F_{V_{stat}\neq 0,Q=0}$ and $F_{V_{stat}=0,Q\neq 0}$), normalized by twice the capacitive force $F_{V_{stat}\neq 0,Q=0}$. Equation (3) is also independent of the value of V_{stat} used to compute the static forces. In the case of FM-KFM, electrostatic forces have to be replaced by electrostatic force gradients. The surface potential $V_{dc}|_{FM-KFM,A=0}$ for an FM-KFM loop with zero tip oscillation (A=0) becomes

$$V_{dc}|_{FM-KFM,A=0}=-V_{stat}\times[F'_{V_{stat}\neq 0,Q\neq 0}-F'_{V_{stat}\neq 0,Q=0}-F'_{V_{stat}=0,Q\neq 0}]/2F'_{V_{stat}\neq 0,Q=0} \quad (4)$$

in which derivatives are taken as a function of z.

To illustrate side-capacitance effects and the use of Eqs. (3) and (4), we performed numerical simulations using COMSOL as Poisson solver, in axial symmetry. We show in Figs. 1(a) and 1(b) the geometry and the local isopotential pattern of a charged disk (diameter d, charge density ρ) within a disk-shape dielectric layer ($\varepsilon_r=4$) of fixed height $h=10$ nm laying on a metal substrate, and probed by a metallic tip (of same work function as the metal substrate). A tip apex of 25 nm and a cone half angle of 15° has been used. In order to minimize computational resources, we introduced an effective description for the cantilever, of disk shape, diameter 2.9 μm, and placed at a 1.0 μm distance above the substrate plane. This configuration reproduces the typical capacitance gradient (here 5.4×10^{-11} F/m) of a commercial cantilever.[13] Von Neumann boundary conditions have been taken at the edge of the simulation box. Results plotted in Fig. 1(c) correspond to the dc surface potential calculated using Eqs. (3) and (4), and normalized with respect to the $\rho h^2/2\varepsilon_0\varepsilon_r$ value of the surface potential of a homogeneously charged dielectric layer of height h and charge density ρ.[14] This value is reached in Fig. 1(c) when using a cantilever without tip and a homogenously charged dielectric layer ($d=2.9$ μm) independently of the cantilever-substrate distance.

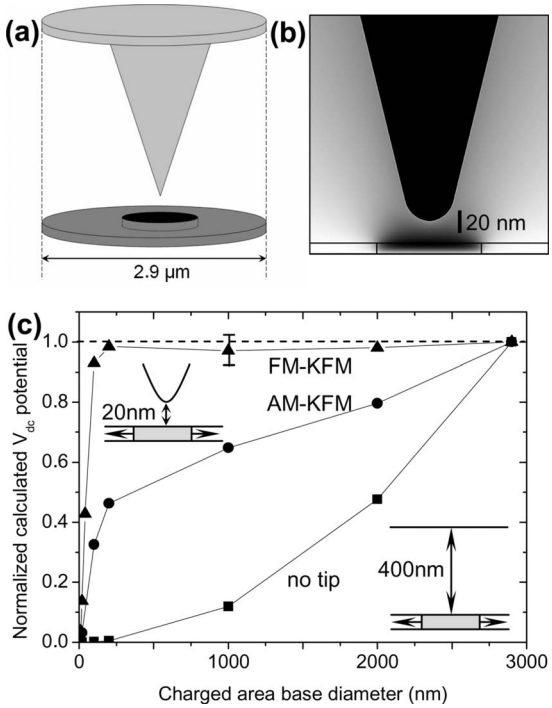

FIG. 1. (a) Schematics of the tip-substrate geometry in axial symmetry. A spherical-conical tip with disk-shape cantilever is used. (b) Zoom-in of the isopotential pattern of the tip probing a charged disk (diameter $d=100$ nm) within a dielectric layer of thickness 10 nm and relative dielectric constant $\varepsilon=4$. The tip and metal surface are grounded. (c) Plot of the surface potential of the charged disk as a function of its diameter d. The limit of $d=2.9$ μm corresponds to a homogeneously charged dielectric layer. The surface potential is normalized by that of the homogeneously charged dielectric layer (see text), and plotted either for a cantilever without tip (squares), and for AM-KFM (circles) and FM-KFM (triangles).

When probing (also without tip) a charged area of diameter $d<2.9$ μm within the dielectric layer, the normalized surface potential measured by the KFM loop is reduced, and shows a parabolic variation with respect to d, i.e., a proportionality with the disk surface, as expected from a side-capacitance effect[4] in a plane capacitor geometry. When a tip is now introduced, the normalized surface potential is enhanced at low d due to the stronger weight associated with the tip apex/cone capacitance gradient. This effect is however limited in AM-KFM, and the normalized surface potential does not exceed a few tens of percent for a charged area falling below the tip cone (here $d<500$ nm). Side-capacitance effects effect associated with the cantilever itself thus play a significant role in the interpretation of AM-KFM measurements.[5] We also plotted in Fig. 1(c) the calculated dc potential in the case of FM-KFM, using Eq. (4). The normalized surface potential is seen to increase rapidly toward unity for $0\leq d\leq 200$ nm, meaning that side-capacitance effects associated with the cantilever itself are here negligible.[13] The error bars correspond here to the uncertainty introduced by the calculation of the force derivatives in Eq. (4).

We now investigate the case of an oscillating tip-probe ($A\neq 0$),[2,3,11,12] together with the sample topography acquired in dynamic mode.[3] Our model can be easily extended to this situation, by considering the time-evolution of Eq. (2). Since the KFM regulation loop bandwidth stays low as compared to the cantilever oscillation frequency,[11,15] the force components in Eq. (2) simply become integrated over time. This leads to the following formula for surface potentials in AM

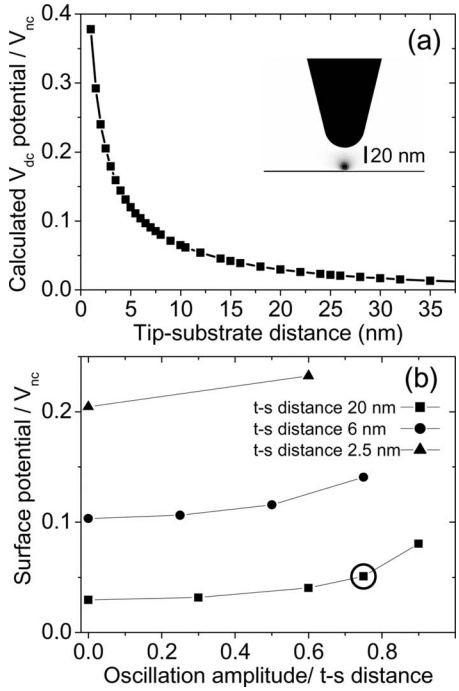

FIG. 2. (a) Surface potential of a charged dielectric sphere (relative dielectric constant $\varepsilon=12$) of diameter 8 nm, normalized with respect to the volume average V_{nc} of the charged sphere electrostatic potential, and represented as a function of the tip-sample distance z. Inset: Isopotential pattern for $z=20$ nm, and a grounded tip and substrate. (b) Calculated AM-KFM surface potential (normalized with respect to V_{nc}) in the case of an oscillating tip, and for three average tip-sample (t-s) distance ($\langle z\rangle=20$ nm, 6 nm, and 2.5 nm), and plotted as a function of the normalized tip oscillation amplitude $A/\langle z\rangle$. The surrounded point corresponds to a tip oscillation amplitude $A=15$ nm and a minimum tip-substrate distance of 5 nm.

or FM modes for a nonzero tip oscillation ($A\neq 0$) using integrals over a cantilever oscillation period

$$V_{dc}|_{AM-KFM,A\neq 0} = -V_{stat}\times\left[\int F_{V_{stat}\neq 0,Q\neq 0}dt - \int F_{V_{stat}\neq 0,Q=0}dt - \int F_{V_{stat}=0,Q\neq 0}dt\right]/2\int F_{V_{stat}\neq 0,Q=0}dt, \quad (5)$$

$$V_{dc}|_{FM-KFM,A\neq 0} = -V_{stat}\times\left[\int F'_{V_{stat}\neq 0,Q\neq 0}dt - \int F'_{V_{stat}\neq 0,Q=0}dt - \int F'_{V_{stat}=0,Q\neq 0}dt\right]/2\int F'_{V_{stat}\neq 0,Q=0}dt. \quad (6)$$

In these expressions, the time integrals (or force gradient) component can also be replaced by weighted integrals as a function of the tip-substrate distance z, following the approach of Ref. 16. The integrals in Eqs. (5) and (6) play a significant role provided the force or force gradients expressions in Eqs. (3) and (4) exhibit a nonlinear behavior with respect to the tip-substrate distance z, which occurs, e.g., when scanning with rather short tip substrate distances, as in noncontact atomic force microscopy. To illustrate this effect, we show in Fig. 2(a) the surface potential V_{dc} which would be regulated by AM-KFM over a charged dielectric sphere (height 8 nm, charge density $+10^{18}e$ cm^{-3}, $\varepsilon=12$), as a function of the distance z between the tip apex and charged sphere, and with no tip oscillation ($A=0$). V_{dc} has been here normalized with respect to the volume average V_{nc} of the charged sphere electrostatic potential and shows values up to a few tens percents, as previously discussed. A clear nonlinear behavior is visible from Fig. 2(a). It stems (i) from the nonlinearities of local Coulomb forces or force gradients and (ii) from the intrinsic z-dependence of side-capacitance effects.[4] The impact of nonlinearities however depends in practice on both the average tip-substrate distance $\langle z\rangle$ and on the tip-oscillation amplitude A. This is further illustrated in Fig. 2(b), in which the normalized surface potential over the charged dielectric sphere has been calculated for an AM-KFM loop using Eq. (5) for three different average tip-substrate distances ($\langle z\rangle=20$ nm, 6 nm, and 2.5 nm), and as a function of the tip oscillation amplitude (here normalized with respect to $\langle z\rangle$). The V_{dc} potential regulated by the KFM loop is seen to increase when $\langle z\rangle$ is decreased, in agreement with Fig. 2(a), but also to increase with the tip oscillation amplitude, as a result of the nonlinearities. The weight of nonlinear effects in AM-KFM (or FM-KFM) has in practice to be determined carefully from scanning conditions, with the aim to obtain a quantitative interpretation of KFM experiments.

In conclusion, we have established a formula to calculate KFM signals from static force fields, which can be used either for AM-KFM or FM-KFM. This general model can be conveniently used to take into account side-capacitance and nonlinear effects, so as to extract quantitative information from KFM signals at the nanometer or atomic scales.

We thank H. Diesinger, D. Deresmes, and ANR for support under Contract No. ANR 06-NANO-070.

[1] M. Nonnenmacher, M. P. O'Boyle, and H. K. Wickramasinghe, Appl. Phys. Lett. **58**, 2921 (1991).
[2] See, e.g., A. Kikukawa, S. Hosaka, and R. Imura, Appl. Phys. Lett. **66**, 3510 (1995).
[3] See, e.g., D. Ziegler, J. Rychen, N. Naujoks, and A. Stemmer, Nanotechnology **18**, 225505 (2007).
[4] H. O. Jacobs, P. Leuchtmann, O. J. Homan, and A. Stemmer, J. Appl. Phys. **84**, 1168 (1998).
[5] D. S. H. Charrier, M. Kemerink, B. E. Smalbrugge, T. de Vries, and R. A. J. Janssen, ACS Nano **2**, 622 (2008).
[6] S. Sadewasser, Th. Glatzel, R. Shikler, Y. Rosenwaks, and M. Ch. Lux-Steiner, Appl. Surf. Sci. **210**, 32 (2003).
[7] F. Krok, K. Sajewicz, J. Konior, M. Goryl, P. Platkowski, and M. Szymonski, Phys. Rev. B **77**, 235427 (2008).
[8] T. Glatzel, L. Zimmerli, S. Koch, B. Such, S. Kawai, and E. Meyer, Nanotechnology **20**, 264016 (2009).
[9] D. Brunel, D. Deresmes, and T. Mélin, Appl. Phys. Lett. **94**, 223508 (2009).
[10] L. Nony, A. S. Foster, F. Bocquet, and C. Loppacher, Phys. Rev. Lett. **103**, 036802 (2009).
[11] T. Glatzel, S. Sadewasser, and M. C. Lux-Steiner, Appl. Surf. Sci. **210**, 84 (2003).
[12] U. Zerweck, C. Loppacher, T. Otto, S. Grafström, and L. M. Eng, Phys. Rev. B **71**, 125424 (2005).
[13] We used for FM-KFM simulations the same cantilever description as for AM-KFM simulations. This is strictly speaking improper, because the effective cantilever should be chosen in FM-KFM in order to match the experimental values for the cantilever-substrate second capacitance derivative. Side-capacitance effects associated with the cantilever have therefore been overestimated by a factor 10–15 in the FM-KFM simulations of Fig. 1. This however does not play any role here since their effect is negligible.
[14] T. Mélin, H. Diesinger, D. Deresmes, and D. Stiévenard, Phys. Rev. B **69**, 035321 (2004).
[15] H. Diesinger, D. Deresmes, J.-P. Nys, and T. Mélin, Ultramicroscopy **110**, 162 (2010).
[16] F. J. Giessibl, Phys. Rev. B **56**, 16010 (1997).